A generalized time-domain framework for modeling and analysis of the unbalanced three-phase systems

Ali Tayyebi
Dierk Bormann
Hitachi Energy Research
Västerås, Sweden
{ali.tayyebi}@hitachienergy.com

Weichi Zhang
Helen-Xing Huang
Wene-Wen Jiang
Hitachi Energy Research
Beijing, China

Mats Larsson
Hitachi Energy Research
Baden-Daettwil, Switzerland

***Abstract*—This paper provides the theoretic foundation of a new time-domain modeling framework for three-phase unbalanced AC power systems. In particular, a generalized variant of the standard dq0 transformation termed as g-dq0 transform is derived. The proposed g-dq0 transform represents any phase and/or magnitude unbalanced three-phase quantity in a time-invariant coordinates system, thus replicating the features of standard dq0 transform for balanced AC systems. Furthermore, underpinned by an invariance-preserving property, the g-dq0 transform projects impedance and admittance matrices onto an equivalent time-invariant representation regardless of the structural asymmetry or imbalances in time-domain quantities. Finally, we provide an example for the dynamic circuit modeling in g-dq0 coordinates, modeling details on different unbalanced load configurations, and simulation-based accuracy verification test cases.**

***Index Terms*—power system, power converter, unbalanced AC systems, Park transformation, Clarke transformation.**

I. Introduction

The global shift toward integration of renewable energy sources due to the climate change concerns has been transforming the power grid to a so-called converter-dominated state. This is due to fact that the renewable energy sources are predominantly interfaced with the grid via power electronics converter. The replacement of well-established synchronous machine (SM) technologies (and their stabilizing control mechanisms) with power converters poses critical stability and robustness challenges for the power system operation. Therefore, designing new converter control methods, establishing new modeling and simulation frameworks, performing stability and interaction analysis, and redefining grid codes and test requirements are currently and extensively being explored by the academic community, manufacturers, and system operators [1]–[9].

An open problem associated with the converter-based systems is the rigorous modeling and analysis of the unbalanced system to ensure a robust and reliable operation. Unbalanced conditions in a converter-dominated power grid can occur in several potential scenarios, e.g., single-phase small-scale microgrid applications, system- and device-level unbalanced fault conditions, unbalanced load integration, and non-uniform per-phase parameter tolerances, among others. It is worth mentioning that establishing accurate and generic modeling framework for the unbalanced system dynamics is a prerequisite for the control design and stability analysis of such systems.

The aforementioned problem was previously explored along several directions, e.g., by exploiting dynamic phasor theory [10], independent reciprocal basis theory [11], symmetrical component system theory [12], [13], and time-domain modeling frameworks [14], [15]. However, to the best of our knowledge a linear time-invariant representation of unbalanced system dynamics in presence of phase-and-magnitude unbalanced AC quantities and asymmetric three-phase circuitry is an open problem to this date. In this paper, we extend the transformation proposed in [14], and derive a generalized time-domain transformation for the unbalanced system. The proposed transformation resembles and extends the standard dq0 transform (that is broadly utilized in modeling and analysis of the balanced AC systems [16]–[19]), thus, it is termed as the generalized dq0, i.e., g-dq0 transform.

In this work, we begin by establishing the g-dq0 transform for the magnitude-unbalanced AC signals (which is centered around the unbalanced signal consideration). We continue by highlighting the transform application for the phase-unbalanced signals, as well. Next, we present details on the properties of the g-dq0 transform, derive its inverse, prove an invariance-preserving property under the g-dq0 transform, and subsequently show how it can be utilized to transform electrical circuit dynamics (that is centered around the unbalanced circuit parameter consideration). Finally, we provide an example for the dynamic circuit modeling in g-dq0 coordinates, modeling details on different unbalanced load configurations, and simulation-based accuracy verification test cases (that simultaneously include unbalanced signals and circuit parameters).

II. Theoretical Foundation

In this section, we establish the theoretic foundation of the g-dq0 transform. For the sake of completeness, we firstly follow

Submitted to the 23rd Power Systems Computation Conference (PSCC 2024).

the recipe in [14] to derive an intermediate transformation that is subsequently extended to the g-dq0 transform.

A. Notation and preliminaries

In this paper, $\mathbb{R}$ denotes the set of real numbers, $\mathbb{R}_{>0}$ denotes the set of positive real numbers, and $\mathbb{R}_{[a,b]}$ denotes the interval between real numbers a and b. The square matrix of all zeros is denoted by $\mathbf{0}_{n\times n}$, the n-dimensional identity matrix and column vector of all ones are denoted by $\mathbf{I}_n$ and $\mathbb{1}_n$, respectively. For the column vectors $y_m \in \mathbb{R}^m$ and $y_n \in \mathbb{R}^n$, $y = (y_m, y_n) \in \mathbb{R}^{m+n}$ denotes the stacked column vector. Next, $y(t) \in \mathbb{R}^m$ and $y_{\text{abc}}(t) \in \mathbb{R}^3$ respectively denote a m-dimensional non-three-phase and three-dimensional three-phase quantities at time $t > 0$.

A generic three-phase quantity is defined by

$$y_{\text{abc}}(t) := \begin{pmatrix} y_{\text{a}}(t) \\ y_{\text{b}}(t) \\ y_{\text{c}}(t) \end{pmatrix} = \begin{pmatrix} Y_{\text{a}} \cos\left(\theta_{\text{a}}(t) + \delta_{\text{a}}\right) \\ Y_{\text{b}} \cos\left(\theta_{\text{b}}(t) + \delta_{\text{b}}\right) \\ Y_{\text{c}} \cos\left(\theta_{\text{c}}(t) + \delta_{\text{c}}\right) \end{pmatrix}, \tag{1}$$

where Y_{a}, Y_{b}, and $Y_{\text{c}} \in \mathbb{R}_{>0}$ denote the per-phase magnitudes that are not necessarily identical,

$$\begin{pmatrix} \theta_{\text{a}}(t) \\ \theta_{\text{b}}(t) \\ \theta_{\text{c}}(t) \end{pmatrix} = \begin{pmatrix} \omega^\star t \\ \omega^\star t - \frac{2\pi}{3} \\ \omega^\star t + \frac{2\pi}{3} \end{pmatrix}, \tag{2}$$

denotes a set of three-phase balanced phase angles in which $\omega^\star \in \mathbb{R}_{>0}$ denote the stationary angular frequency and δ_{a}, δ_{b}, and $\delta_{\text{c}} \in \mathbb{R}_{[0,2\pi]}$ denote arbitrary constant phase angle shifts.

The magnitude-preserving Clarke (i.e., abc $\to \alpha\beta\gamma$) transformation [20] and Park (i.e., $\alpha\beta\gamma \to$ dq0) coordinate transformation are respectively defined by

$$\mathbf{T}_{\text{Clarke}} = \frac{2}{3} \begin{pmatrix} 1 & -\frac{1}{2} & -\frac{1}{2} \\ 0 & \frac{\sqrt{3}}{2} & -\frac{\sqrt{3}}{2} \\ \frac{1}{2} & \frac{1}{2} & \frac{1}{2} \end{pmatrix}, \tag{3}$$

and

$$\mathbf{T}_{\text{Park}}(\cdot) = \begin{pmatrix} \cos(\cdot) & \sin(\cdot) & 0 \\ -\sin(\cdot) & \cos(\cdot) & 0 \\ 0 & 0 & 1 \end{pmatrix}. \tag{4}$$

Last, $\partial/\partial t$ denotes the partial derivative with respect to time.

B. The generalized dq0 transform

We begin by considering the following three-phase time-dependent quantity

$$x_{\text{abc}}(t) = \begin{pmatrix} x_{\text{a}}(t) \\ x_{\text{b}}(t) \\ x_{\text{c}}(t) \end{pmatrix} = \begin{pmatrix} X_{\text{a}} \cos\theta_{\text{a}}(t) \\ X_{\text{b}} \cos\theta_{\text{b}}(t) \\ X_{\text{c}} \cos\theta_{\text{c}}(t) \end{pmatrix}, \tag{5}$$

in which the phase magnitudes are not necessarily identical[1]. Let us consider the diagonal augmentation of the Clarke transformation introduced in Subsection II-A, that is,

$$\underline{\mathbf{T}}_{\text{Clarke}} = \begin{pmatrix} \mathbf{T}_{\text{Clarke}} & \mathbf{0}_{3\times 3} \\ \mathbf{0}_{3\times 3} & \mathbf{T}_{\text{Clarke}} \end{pmatrix}. \tag{6}$$

[1]The case with the arbitrary phase angle shifts is discussed later

Similarly, one can define rotation angles for the standard Park transformation (as in Subsection II-A) in positive and negative directions and subsequently, augment $\alpha\beta\gamma \to$ dq0 coordinates transformation as

$$\underline{\mathbf{T}}_{\text{Park}} = \begin{pmatrix} \mathbf{T}_{\text{Park}}\left(\omega^\star t\right) & \mathbf{0}_{3\times 3} \\ \mathbf{0}_{3\times 3} & \mathbf{T}_{\text{Park}}\left(-\omega^\star t\right) \end{pmatrix}. \tag{7}$$

Next, we apply the signal delay cancellation method as in [14], [21] that is the time-domain equivalent of the standard Fortescue transformation [13]. The transformation matrix associated with the signal delay cancellation method takes the form [14]

$$\mathbf{T}_{+-0} = \frac{1}{2} \begin{pmatrix} 1 & 0 & 0 & 0 & -1 & 0 \\ 0 & 1 & 0 & 1 & 0 & 0 \\ 0 & 0 & 1 & 0 & 0 & 0 \\ 1 & 0 & 0 & 0 & 1 & 0 \\ 0 & 1 & 0 & -1 & 0 & 0 \\ 0 & 0 & 0 & 0 & 0 & 1 \end{pmatrix}. \tag{8}$$

Last, we introduce the time-delayed copies of the original signal in (5) as

$$x_{\text{abc}}(t-\tau) = \begin{pmatrix} x_{\text{a}}(t-\tau) \\ x_{\text{b}}(t-\tau) \\ x_{\text{c}}(t-\tau) \end{pmatrix} = \begin{pmatrix} X_{\text{a}} \cos\theta_{\text{a}}(t-\tau) \\ X_{\text{b}} \cos\theta_{\text{b}}(t-\tau) \\ X_{\text{c}} \cos\theta_{\text{c}}(t-\tau) \end{pmatrix}, \tag{9}$$

where $\tau = \pi/2\omega^\star$ denotes the quarter-period of the periodic signals in (5) and let

$$\underline{x}_{\text{abc}}(t) = \begin{pmatrix} x_{\text{abc}}(t) \\ x_{\text{abc}}(t-\tau) \end{pmatrix}. \tag{10}$$

Having all the preliminaries in place, below composite transformation projects the original signal (5) and its delayed copy (9) onto a six-dimensional coordinate system that comprises the positive and negative components for the dq0 coordinates, i.e.,

$$\begin{aligned} x^{\pm}_{\text{dq0}}(t) &= \underline{\mathbf{T}}_{\text{Park}} \mathbf{T}_{+-0} \underline{\mathbf{T}}_{\text{Clarke}} \underline{x}_{\text{abc}}(t) \\ &= \begin{pmatrix} x^+_{\text{d}} \\ x^+_{\text{q}} \\ x^+_0 \\ x^-_{\text{d}} \\ x^-_{\text{q}} \\ x^-_0 \end{pmatrix} = \begin{pmatrix} \kappa^+_{\text{d}}\left(X_{\text{a}} + X_{\text{b}} + X_{\text{c}}\right) \\ 0 \\ \kappa^+_0\left(x^\top_{\text{abc}}(t)\mathbb{1}_3\right) \\ \kappa^-_{\text{d}}\left(2X_{\text{a}} - X_{\text{b}} - X_{\text{c}}\right) \\ \kappa^-_{\text{q}}\left(X_{\text{c}} - X_{\text{b}}\right) \\ \kappa^-_0\left(x^\top_{\text{abc}}(t-\tau)\mathbb{1}_3\right) \end{pmatrix}, \end{aligned} \tag{11}$$

where $(\kappa^+_{\text{d}}, \kappa^+_0, \kappa^-_{\text{d}}, \kappa^-_{\text{q}}, \kappa^-_0) = (1/6)\left(2, 1, 1, \sqrt{3}, 1\right)$.

Assumption 1 (Stationary angular frequency)
We assume that all three-phase quantities are constrained to a stationary angular frequency $\omega^\star$.

The implication of the Assumption 1 is that the presented coordinate transformations are applicable to the steady-state three-phase quantities, thus, delivering a steady-state model of the unbalanced systems, as in [14]. More precisely, all the AC signals are assumed to be in a steady-state condition with a constant frequency.

Remark 1 (Intermediate coordinate transformation [14])
Under the balanced signal condition, i.e., $X_{\text{a}} = X_{\text{b}} = X_{\text{c}}$

in (5) *and* (9) *all the elements of* $x^{\pm}_{\text{dq0}}(t)$ *in* (11) *vanish except* $x^{+}_{\text{d}} = X_{\text{a}}$. *Therefore, the coordinate transformation* $\underline{\mathbf{T}}_{\text{Park}}\mathbf{T}_{+-0}\underline{\mathbf{T}}_{\text{Clarke}}$ *is magnitude-preserving that follows from the choice of Clarke transformation* $\mathbf{T}_{\text{Clarke}}$ *in* (3). *Under the unbalanced signal condition (i.e., the general case), although the image of the unbalanced three-phase quantity* (5) *as in* (11) *includes four time-invariant elements, the* $x^{\pm}_{0}$ *coordinates are still time-varying.*

In what follows, we extend the coordinate transformation in (11) such that all target coordinates are time-invariant. It is worth mentioning that a time-invariant representation of the unbalanced three-phase quantities allows to apply standard linear modeling, analysis, and control design tools to unbalanced three-phase systems.

Proposition 1 (Linear combination of sinusoids)
For a set of sinusoids with an identical frequency and arbitrary magnitudes and phase shifts, the following identity holds

$$\sum_{j=1}^{n} Y_j \cos\left(\omega t + \phi_j\right) = Y\cos\left(\omega t + \phi\right), \tag{12}$$

where n *is a positive integer and* Y *and* ϕ *are given by*

$$Y = \sqrt{\left(\sum_{j=1}^{n} Y_j \cos\phi_j\right)^2 + \left(\sum_{j=1}^{n} Y_j \sin\phi_j\right)^2}, \tag{13a}$$

$$\phi = \tan^{-1}\left(\frac{\sum_{j=1}^{n} Y_j \sin\phi_j}{\sum_{j=1}^{n} Y_j \cos\phi_j}\right). \tag{13b}$$

Proof is provided in the Appendix. Note that the time-varying coordinates in (11), i.e., x^{+}_{0} and x^{-}_{0} (similar to the left-hand side (LHS) of (12)) are linear combinations of the cosine functions in (5) and (9), respectively. Therefore, by applying Proposition 1 one can alternatively write x^{+}_{0} and x^{-}_{0} in (11) as

$$\begin{pmatrix} x^{+}_{0} \\ x^{-}_{0} \end{pmatrix} = \kappa_0 X_0 \begin{pmatrix} \cos\left(\omega^{\star} t + \phi_0\right) \\ \sin\left(\omega^{\star} t + \phi_0\right) \end{pmatrix}, \tag{14}$$

where $\kappa_0 = \kappa^{+}_{0} = \kappa^{-}_{0}$, and X_0 and ϕ_0 are respectively defined by (13a) and (13b) with $Y_j \in \{X_{\text{a}}, X_{\text{b}}, X_{\text{c}}\}$ and $\phi_j \in \{0, \pm 2\pi/3\}$. It is worth mentioning that the sine term in (14) arises due to the time-delayed nature of x^{-}_{0} as in (11).

Note that the image of an arbitrary three-phase balanced quantity (e.g., as in (5) while assuming $X_{\text{a}} = X_{\text{b}} = X_{\text{c}}$) in the stationary $\alpha\beta\gamma$-coordinates (established by $\mathbf{T}_{\text{Clarke}}$ as in Subsection II-A) includes sine, cosine, and zero components. Thus, the combination of x^{+}_{0} and x^{-}_{0} in (14) and x^{+}_{q} in (11), can be perceived as the image of a three-phase balanced quantity in $\alpha\beta\gamma$-coordinates. Inspired by this observation, we replace x^{+}_{0} and x^{-}_{0} in (11) by the expressions in (14) and introduce the permutation matrix

$$\mathbf{T}_{\text{P}} = \begin{pmatrix} 1 & 0 & 0 & 0 & 0 & 0 \\ 0 & 0 & 0 & 1 & 0 & 0 \\ 0 & 0 & 0 & 0 & 1 & 0 \\ 0 & 0 & 1 & 0 & 0 & 0 \\ 0 & 0 & 0 & 0 & 0 & 1 \\ 0 & 1 & 0 & 0 & 0 & 0 \end{pmatrix}, \tag{15}$$

that subsequently reorders the coordinates of (11) to

$$\mathbf{T}_{\text{P}} x^{\pm}_{\text{dq0}}(t) = \begin{pmatrix} \kappa^{+}_{\text{d}}\left(X_{\text{a}} + X_{\text{b}} + X_{\text{c}}\right) \\ \kappa^{-}_{\text{d}}\left(2X_{\text{a}} - X_{\text{b}} - X_{\text{c}}\right) \\ \kappa^{-}_{\text{q}}\left(X_{\text{c}} - X_{\text{b}}\right) \\ \kappa_0 X_0 \cos\left(\omega^{\star} t + \phi_0\right) \\ \kappa_0 X_0 \sin\left(\omega^{\star} t + \phi_0\right) \\ 0 \end{pmatrix}. \tag{16}$$

Next, we construct an auxiliary transformation that respectively preserves the time-invariant and rotates the time-varying elements in (16), that is,

$$\mathbf{T}_{\text{R}} = \begin{pmatrix} \mathbf{I}_3 & \mathbf{0}_{3\times 3} \\ \mathbf{0}_{3\times 3} & \mathbf{T}_{\text{Park}}\left(\omega^{\star} t\right) \end{pmatrix}. \tag{17}$$

Finally, combining (6)-(8), (15), and (17) establishes a composite mapping, i.e., the generalized dq0 transform

$$\boxed{\mathbf{M} = \mathbf{T}_{\text{R}}\mathbf{T}_{\text{P}}\underline{\mathbf{T}}_{\text{Park}}\mathbf{T}_{+-0}\underline{\mathbf{T}}_{\text{Clarke}},} \tag{18}$$

that transforms $\underline{x}_{\text{abc}}(t)$ in (10) to a time-invariant form

$$\boxed{x_{\text{g-dq0}} = \mathbf{M}\underline{x}_{\text{abc}}(t) = \begin{pmatrix} \kappa^{+}_{\text{d}}\left(X_{\text{a}} + X_{\text{b}} + X_{\text{c}}\right) \\ \kappa^{-}_{\text{d}}\left(2X_{\text{a}} - X_{\text{b}} - X_{\text{c}}\right) \\ \kappa^{-}_{\text{q}}\left(X_{\text{c}} - X_{\text{b}}\right) \\ \kappa_0 \cos(\phi_0) X_0 \\ \kappa_0 \sin(\phi_0) X_0 \\ 0 \end{pmatrix}.} \tag{19}$$

For the clarity of exposition $\mathbf{M}$ is expanded as in (20)[2]. We close this section by remarking that the target coordinates (19) are time-invariant when the original signal in (5) is in steady state. Therefore, one can apply the representation (19) for the small-signal modeling, stability analysis, and control design of the unbalanced systems.

III. Properties and Applications

In this section, we investigate the properties of coordinate transformation (18) and show how it can be applied to model circuit dynamics.

A. Generalized dq0 transform properties

To begin with, let us highlight a fundamental similarity between (18) and the standard dq0 transformation [19], [20] that is widely recognized as a powerful tool for the modeling, analysis, and control of the balanced AC systems.

The standard Park transformation as in [20] that is obtained by combining the Clarke (3) and dq0 transforms (4), projects a set of steady-state three-phase (phase and magnitude) balanced quantity onto a three-dimensional time-invariant representation. If the axes of the rotating dq0-frame are appropriately aligned with the those of the original abc-frame, then the resulting quantity in dq0-coordinates has only one non-zero element. This is the direct consequence of the fact that a three-phase balanced AC quantity is fully represented by its magnitude at a prescribed frequency.

[2]Due to the lengthy calculations required to derive (20), we recommend the interested reader to possibly evaluate (20) with a symbolic computational tool, as well.

$$\mathbf{M}=\frac{1}{3}\begin{pmatrix}\cos(\omega^\star t) & -\cos\left(\omega^\star t+\frac{\pi}{3}\right) & -\cos\left(\omega^\star t-\frac{\pi}{3}\right) & \sin(\omega^\star t) & -\sin\left(\omega^\star t+\frac{\pi}{3}\right) & \cos\left(\omega^\star t+\frac{\pi}{6}\right)\\ \cos(\omega^\star t) & -\cos\left(\omega^\star t-\frac{\pi}{3}\right) & -\cos\left(\omega^\star t+\frac{\pi}{3}\right) & \sin(\omega^\star t) & \cos\left(\omega^\star t+\frac{\pi}{6}\right) & -\sin\left(\omega^\star t+\frac{\pi}{3}\right)\\ \sin(\omega^\star t) & \cos\left(\omega^\star t+\frac{\pi}{6}\right) & -\sin\left(\omega^\star t+\frac{\pi}{3}\right) & -\cos(\omega^\star t) & \cos\left(\omega^\star t-\frac{\pi}{3}\right) & \cos\left(\omega^\star t+\frac{\pi}{3}\right)\\ \frac{1}{2}\cos(\omega^\star t) & \frac{1}{2}\cos(\omega^\star t) & \frac{1}{2}\cos(\omega^\star t) & \frac{1}{2}\sin(\omega^\star t) & \frac{1}{2}\sin(\omega^\star t) & \frac{1}{2}\sin(\omega^\star t)\\ -\frac{1}{2}\sin(\omega^\star t) & -\frac{1}{2}\sin(\omega^\star t) & -\frac{1}{2}\sin(\omega^\star t) & \frac{1}{2}\cos(\omega^\star t) & \frac{1}{2}\cos(\omega^\star t) & \frac{1}{2}\cos(\omega^\star t)\\ -\sin(\omega^\star t) & \sin\left(\omega^\star t+\frac{\pi}{3}\right) & -\cos\left(\omega^\star t+\frac{\pi}{6}\right) & \cos(\omega^\star t) & -\cos\left(\omega^\star t+\frac{\pi}{3}\right) & -\cos\left(\omega^\star t-\frac{\pi}{3}\right)\end{pmatrix}. \quad (20)$$

Similarly, the coordinate transformation (18) transforms an unbalanced three-phase quantity into a six-dimensional time-invariant representation. Note that a general three-phase quantity (with unbalanced phase and magnitude) as in (1) is defined by six independent quantity (i.e., the magnitudes and phase angles) at a certain frequency. Therefore, the transform in (18) can be perceived as the generalized form of the standard dq0 transformation. Next remark demonstrates that the transformation $\mathbf{M}$ in (18) is invertible, therefore, one can uniquely recover the original signals from the target coordinates (19).

Remark 2 (Inverse g-dq0 transform)
Straightforward computations shows that all the underlying transformations in the right-hand side (RHS) of (18) *are invertible. Therefore, the inverse g-dq0 transform is given by*

$$\mathbf{M}^{-1}=\underline{\mathbf{T}}^{-1}_{\text{Clarke}}\mathbf{T}^{-1}_{+-0}\underline{\mathbf{T}}^{-1}_{\text{Park}}\mathbf{T}^{-1}_{\text{P}}\mathbf{T}^{-1}_{\text{R}}. \quad (21)$$

The coordinates transformation (18) in Section II is derived while considering magnitude-unbalanced AC quantities. In what follows, we extend the transformation application to the phase-unbalanced AC quantities. Consider the general AC signal form in (1) that is alternatively written as

$$y_{\text{abc}}=y_{\text{abc},1}-y_{\text{abc},2}=\begin{pmatrix}\tilde{Y}_{\text{a}}\cos\theta_{\text{a}}\\ \tilde{Y}_{\text{b}}\cos\theta_{\text{b}}\\ \tilde{Y}_{\text{c}}\cos\theta_{\text{c}}\end{pmatrix}-\begin{pmatrix}\hat{Y}_{\text{a}}\sin\theta_{\text{a}}\\ \hat{Y}_{\text{b}}\sin\theta_{\text{b}}\\ \hat{Y}_{\text{c}}\sin\theta_{\text{c}}\end{pmatrix}, \quad (22)$$

where we exploited the trigonometric angle sum identity, and

$$\begin{pmatrix}\tilde{Y}_{\text{a}}\\ \tilde{Y}_{\text{b}}\\ \tilde{Y}_{\text{c}}\end{pmatrix}=\begin{pmatrix}Y_{\text{a}}\cos\delta_{\text{a}}\\ Y_{\text{b}}\cos\delta_{\text{b}}\\ Y_{\text{c}}\cos\delta_{\text{c}}\end{pmatrix}\quad\text{and}\quad\begin{pmatrix}\hat{Y}_{\text{a}}\\ \hat{Y}_{\text{b}}\\ \hat{Y}_{\text{c}}\end{pmatrix}=\begin{pmatrix}Y_{\text{a}}\sin\delta_{\text{a}}\\ Y_{\text{b}}\sin\delta_{\text{b}}\\ Y_{\text{c}}\sin\delta_{\text{c}}\end{pmatrix}.$$

Let us shift the angles in (2) and define

$$\begin{pmatrix}\vartheta_{\text{a}}\\ \vartheta_{\text{b}}\\ \vartheta_{\text{c}}\end{pmatrix}=\begin{pmatrix}\theta_{\text{a}}\\ \theta_{\text{b}}\\ \theta_{\text{c}}\end{pmatrix}-\left(\frac{\pi}{2}\right)\mathbb{1}_3. \quad (23)$$

Subsequently, the sine terms in the RHS of (22) are alternatively written as

$$\begin{pmatrix}\hat{Y}_{\text{a}}\sin\theta_{\text{a}}\\ \hat{Y}_{\text{b}}\sin\theta_{\text{b}}\\ \hat{Y}_{\text{c}}\sin\theta_{\text{c}}\end{pmatrix}=\begin{pmatrix}\hat{Y}_{\text{a}}\cos\vartheta_{\text{a}}\\ \hat{Y}_{\text{b}}\cos\vartheta_{\text{b}}\\ \hat{Y}_{\text{c}}\cos\vartheta_{\text{c}}\end{pmatrix}.$$

Therefore, both $y_{\text{abc},1}$ and $y_{\text{abc},2}$ in (22) take a phase-balanced cosine form as in (5). Next, creating $\underline{y}_{\text{abc},1}$ and $\underline{y}_{\text{abc},2}$ according to (10) and applying (19) yields that

$$y_{\text{g-dq0}}=y_{\text{g-dq0},1}-y_{\text{g-dq0},2}=\mathbf{M}\underline{y}_{\text{abc},1}-\mathbf{M}\underline{y}_{\text{abc},2}=\mathbf{M}\underline{y}_{\text{abc}},$$

where $\mathbf{M}$ is given by (18).

B. Dynamic circuit elements representation

Having generalized the application of coordinate transformation $\mathbf{M}$ to the unbalanced AC signals, in what follows, we investigate the representation of the typical parameters in unbalanced electrical circuit, e.g., resistance, inductance, and capacitance in the coordinates established by $\mathbf{M}$. It is noteworthy that the standard dq0 transformation, when applied to symmetric electrical circuits, results in a time-invariant equivalent representation of circuit parameters. In the sequel, we show how the g-dq0 transform replicates this feature of the dq0 transformation for the asymmetric circuits.

Let us begin by establishing a general commutative property under which the circuit parameter matrices are mapped onto a time-invariant representation via an arbitrary transformation.

Proposition 2 (Invariance-preserving property)
Consider a constant square matrix P *and a non-singular differentiable time-varying transformation* $\mathbf{T}$*, if*

$$\left(\frac{\partial\mathbf{T}^{-1}}{\partial t}\mathbf{T}\right)\mathrm{P}=\mathrm{P}\left(\frac{\partial\mathbf{T}^{-1}}{\partial t}\mathbf{T}\right), \quad (24)$$

then $\mathrm{P}_{\mathbf{T}}=\mathbf{T}\mathrm{P}\mathbf{T}^{-1}$ *is constant*[3].

The proof is straightforward, however, for the sake of completeness is provided in the Appendix.

In what follows, we revisit the dynamic model of the resistive-inductive three-phase circuit (note that the dynamic model of the conductive-capacitive three-phase circuits takes a similar form).

To begin with, the dynamics of a typical three-phase RL element in abc-coordinates is given by

$$\mathrm{L}_{\text{abc}}\frac{\mathrm{d}i_{\text{abc}}}{\mathrm{d}t}=v_{1,\text{abc}}-\mathrm{R}_{\text{abc}}i_{\text{abc}}-v_{2,\text{abc}}, \quad (25)$$

where $\mathrm{L}_{\text{abc}}=\mathrm{diag}(L_{\text{a}},L_{\text{b}},L_{\text{c}})$ is assumed to be invertible, $\mathrm{R}_{\text{abc}}=\mathrm{diag}(R_{\text{a}},R_{\text{b}},R_{\text{c}})$, $v_{1,\text{abc}}$, and $v_{2,\text{abc}}$ are three-phase AC quantities with arbitrary magnitudes and phase angle displacements. Note that the phase inductances (and similarly phase resistances) in L_{abc} (and in R_{abc}) do not need to be identical. Thus, we allow for the unbalanced circuit parameters consideration in the forthcoming analysis. Next, let us augment

[3]Note that this is a basic property of any Lie group: if the infinitesimal generator of the transformation $\mathbf{T}$ commutes with P, then $\mathrm{P}_{\mathbf{T}}$ is invariant.

the RL dynamics with the time-delayed copies of the AC quantities as in (10), i.e.,

$$\underline{\mathrm{L}}_{\mathrm{abc}} \frac{\mathrm{d}\underline{i}_{\mathrm{abc}}}{\mathrm{d}t} = \underline{v}_{1,\mathrm{abc}} - \underline{\mathrm{R}}_{\mathrm{abc}} \underline{i}_{\mathrm{abc}} - \underline{v}_{2,\mathrm{abc}}, \tag{26}$$

where $\underline{\mathrm{L}}_{\mathrm{abc}} = \mathrm{diag}(\mathrm{L}_{\mathrm{abc}}, \mathrm{L}_{\mathrm{abc}})$ and $\underline{\mathrm{R}}_{\mathrm{abc}} = \mathrm{diag}(\mathrm{R}_{\mathrm{abc}}, \mathrm{R}_{\mathrm{abc}})$. Subsequently, applying the transformations in (18) and (21) the augmented dynamics (26) take the form in (29). Note that replacing the input/output voltages with input/output currents in (29), the inductor current with capacitor voltage, inductance and resistance matrices with capacitance and conductance matrices allows to model a parallel-connected capacitive-conductive element in a similar fashion. In what follows, we show that the coefficients in the RHS of (29) are time-invariant constant matrices. Note that the coefficients $\mathrm{P}_{\mathbf{M},1}$ and $\mathrm{P}_{\mathbf{M},2}$ in (29) are both in the same form as $\mathrm{P}_{\mathbf{T}}$ in Proposition 2. Some straightforward (albeit lengthy) computation shows that for a generic constant block-diagonal square matrix $\Lambda = \mathrm{diag}(\Lambda_{11}, \Lambda_{11})$ (with similar form as $\underline{\mathrm{L}}_{\mathrm{abc}}^{-1}$ and $\underline{\mathrm{L}}_{\mathrm{abc}}^{-1}\underline{\mathrm{R}}_{\mathrm{abc}}$) as in Proposition 2 and transformation $\mathbf{M}$ as in (18) it holds that

$$\left(\frac{\partial \mathbf{M}^{-1}}{\partial t}\mathbf{M}\right)\Lambda = \Lambda\left(\frac{\partial \mathbf{M}^{-1}}{\partial t}\mathbf{M}\right) = \omega^{\star}\begin{pmatrix}\mathbf{0}_{3\times 3} & -\Lambda_{11}\\ \Lambda_{11} & \mathbf{0}_{3\times 3}\end{pmatrix}.$$

Therefore, the condition of Proposition 2 is satisfied and $\mathrm{P}_{\mathbf{M},1}$, $\mathrm{P}_{\mathbf{M},21}$, and $\mathrm{P}_{\mathbf{M},3}$ in (29) are all constant. Similar computations show that

$$\mathrm{P}_{\mathbf{M},3} = \mathbf{M}\frac{\partial \mathbf{M}^{-1}}{\partial t} = \omega^{\star}\begin{pmatrix}0 & 0 & 0 & 0 & 0 & -1\\ 0 & 0 & 1 & 0 & 0 & 0\\ 0 & -1 & 0 & 0 & 0 & 0\\ 0 & 0 & 0 & 0 & -1 & 0\\ 0 & 0 & 0 & 1 & 0 & 0\\ 1 & 0 & 0 & 0 & 0 & 0\end{pmatrix}.$$

Thus, all the coefficients in the RHS of (29) are time-invariant matrices. Similarly, one can consider a parallel-connected capacitive-conductive element as

$$\mathrm{C}_{\mathrm{abc}} \frac{\mathrm{d}v_{\mathrm{abc}}}{\mathrm{d}t} = i_{1,\mathrm{abc}} - \mathrm{G}_{\mathrm{abc}} v_{\mathrm{abc}} - i_{2,\mathrm{abc}}, \tag{27}$$

where $\mathrm{C}_{\mathrm{abc}} = \mathrm{diag}(C_{\mathrm{a}}, C_{\mathrm{b}}, C_{\mathrm{c}})$ is assumed to be invertible, $\mathrm{G}_{\mathrm{abc}} = \mathrm{diag}(G_{\mathrm{a}}, G_{\mathrm{b}}, G_{\mathrm{c}})$, $i_{1,\mathrm{abc}}$, and $i_{2,\mathrm{abc}}$ are three-phase AC quantities with arbitrary magnitudes and phase angle displacements. Next, the augmented dynamics are given by

$$\underline{\mathrm{C}}_{\mathrm{abc}} \frac{\mathrm{d}\underline{v}_{\mathrm{abc}}}{\mathrm{d}t} = \underline{i}_{1,\mathrm{abc}} - \underline{\mathrm{G}}_{\mathrm{abc}} \underline{v}_{\mathrm{abc}} - \underline{i}_{2,\mathrm{abc}}, \tag{28}$$

where $\underline{\mathrm{C}}_{\mathrm{abc}} = \mathrm{diag}(\mathrm{C}_{\mathrm{abc}}, \mathrm{C}_{\mathrm{abc}})$ and $\underline{\mathrm{G}}_{\mathrm{abc}} = \mathrm{diag}(\mathrm{G}_{\mathrm{abc}}, \mathrm{G}_{\mathrm{abc}})$. Similarly, the augmented dynamics in g-dq0-coordinates are represented by (30). With an analogous procedure one can show that the coefficients in the RHS of (30) are time-invariant, as well.

IV. Circuit Modeling Example

In this section, we provide an example for the dynamic circuit modeling in g-dq0-coordinates. Next, we elaborate on three-phase unbalanced load modeling.

A. Grid-connected converter modeling

We consider a simplified grid-connected power converter that is modeled by an ideal controllable voltage source; see Figure 1 for an illustration. Further, we consider an LC output filter element. Finally, the power grid is modeled with stiff voltage source with an equivalent impedance. Putting all the pieces together, the overall system dynamics in abc-coordinates are described by

$$\mathrm{L}_{\mathrm{abc}} \frac{\mathrm{d}i_{\mathrm{abc}}}{\mathrm{d}t} = v_{\mathrm{c,abc}} - \mathrm{R}_{\mathrm{abc}} i_{\mathrm{abc}} - v_{\mathrm{abc}}, \tag{32a}$$

$$\mathrm{C}_{\mathrm{abc}} \frac{\mathrm{d}v_{\mathrm{abc}}}{\mathrm{d}t} = i_{\mathrm{abc}} - \mathrm{G}_{\mathrm{abc}} v_{\mathrm{abc}} - i_{\mathrm{g,abc}}, \tag{32b}$$

$$\mathrm{L}_{\mathrm{g,abc}} \frac{\mathrm{d}i_{\mathrm{g,abc}}}{\mathrm{d}t} = v_{\mathrm{abc}} - \mathrm{R}_{\mathrm{g,abc}} i_{\mathrm{g,abc}} - v_{\mathrm{g,abc}}, \tag{32c}$$

where the system parameters take the same matrix forms as in (25) and (27), i_{abc} denotes the converter filter inductance current, $v_{\mathrm{c,abc}}$ is the converter voltage behind the filter (that is the control input to the system), v_{abc} is the filter capacitance voltage (i.e., the point of common coupling (PCC) voltage), $i_{\mathrm{g,abc}}$ denotes the grid current, and finally $v_{\mathrm{g,abc}}$ denote the grid voltage, i.e., the physical input to the systems. Next, one can augment the system (32) following a similar approach as in (26) and (28) that results in

$$\underline{\mathrm{L}}_{\mathrm{abc}} \frac{\mathrm{d}\underline{i}_{\mathrm{abc}}}{\mathrm{d}t} = \underline{v}_{\mathrm{c,abc}} - \underline{\mathrm{R}}_{\mathrm{abc}} \underline{i}_{\mathrm{abc}} - \underline{v}_{\mathrm{abc}}, \tag{33a}$$

$$\underline{\mathrm{C}}_{\mathrm{abc}} \frac{\mathrm{d}\underline{v}_{\mathrm{abc}}}{\mathrm{d}t} = \underline{i}_{\mathrm{abc}} - \underline{\mathrm{G}}_{\mathrm{abc}} \underline{v}_{\mathrm{abc}} - \underline{i}_{\mathrm{g,abc}}, \tag{33b}$$

$$\underline{\mathrm{L}}_{\mathrm{g,abc}} \frac{\mathrm{d}\underline{i}_{\mathrm{g,abc}}}{\mathrm{d}t} = \underline{v}_{\mathrm{abc}} - \underline{\mathrm{R}}_{\mathrm{g,abc}} \underline{i}_{\mathrm{g,abc}} - \underline{v}_{\mathrm{g,abc}}. \tag{33c}$$

Finally, by applying the g-dq0 transform (18), we transform the dynamics (33) to a time-invariant representation in g-dq0 coordinates, i.e., (31). Note that all the coefficients in (31) are time-invariant based on construction in Subsection III-B. Further, the unbalances in (31) can possibly originate from non-uniform per-phase parameter tolerances or phase and/or magnitude unbalanced grid voltage. Moreover, in certain scenarios the three-phase converter voltage might be unbalanced, as well; see next section for an example where all the potential unbalanced factors are considered. In the next subsection, we show how the same modeling methodology is applicable when considering star/delta-connected unbalanced loads.

B. Unbalanced load modeling

1) star-connection: let us consider a three-phase RL element that is connected between the phases and ground. The load dynamics in abc-coordinates can be written as

$$\mathrm{L}_{\ell,\mathrm{abc}} \frac{\mathrm{d}i_{\ell,\mathrm{abc}}}{\mathrm{d}t} = \mathrm{S}_{*} v_{\ell,\mathrm{abc}} - \mathrm{R}_{\ell,\mathrm{abc}} i_{\ell,\mathrm{abc}}, \tag{34}$$

where $\mathrm{L}_{\ell,\mathrm{abc}} = \mathrm{diag}(L_{\ell,\mathrm{a}}, L_{\ell,\mathrm{b}}, L_{\ell,\mathrm{c}})$ is assumed to be invertible and $\mathrm{R}_{\ell,\mathrm{abc}} = \mathrm{diag}(R_{\ell,\mathrm{a}}, R_{\ell,\mathrm{b}}, R_{\ell,\mathrm{c}})$, $i_{\ell,\mathrm{abc}}$ denotes the

$$\frac{\mathrm{d}i_{\text{g-dq0}}}{\mathrm{d}t} = \left(\overbrace{\mathbf{M}\underline{\mathrm{L}}_{\text{abc}}^{-1}\mathbf{M}^{-1}}^{=\mathrm{P}_{\mathbf{M},1}}\right) v_{1,\text{g-dq0}} - \left(\overbrace{\mathbf{M}\underline{\mathrm{L}}_{\text{abc}}^{-1}\underline{\mathrm{R}}_{\text{abc}}\mathbf{M}^{-1}}^{=\mathrm{P}_{\mathbf{M},2}} + \overbrace{\mathbf{M}\frac{\partial \mathbf{M}^{-1}}{\partial t}}^{=\mathrm{P}_{\mathbf{M},3}}\right) i_{\text{g-dq0}} - \left(\mathbf{M}\underline{\mathrm{L}}_{\text{abc}}^{-1}\mathbf{M}^{-1}\right) v_{2,\text{g-dq0}}. \tag{29}$$

$$\frac{\mathrm{d}v_{\text{g-dq0}}}{\mathrm{d}t} = \left(\mathbf{M}\underline{\mathrm{C}}_{\text{abc}}^{-1}\mathbf{M}^{-1}\right) i_{1,\text{g-dq0}} - \left(\mathbf{M}\underline{\mathrm{C}}_{\text{abc}}^{-1}\underline{\mathrm{G}}_{\text{abc}}\mathbf{M}^{-1} + \mathbf{M}\frac{\partial \mathbf{M}^{-1}}{\partial t}\right) v_{\text{g-dq0}} - \left(\mathbf{M}\underline{\mathrm{C}}_{\text{abc}}^{-1}\mathbf{M}^{-1}\right) i_{2,\text{g-dq0}}. \tag{30}$$

$$\frac{\mathrm{d}i_{\text{g-dq0}}}{\mathrm{d}t} = \left(\mathbf{M}\underline{\mathrm{L}}_{\text{abc}}^{-1}\mathbf{M}^{-1}\right) v_{\text{c,g-dq0}} - \left(\mathbf{M}\underline{\mathrm{L}}_{\text{abc}}^{-1}\underline{\mathrm{R}}_{\text{abc}}\mathbf{M}^{-1} + \mathbf{M}\frac{\partial \mathbf{M}^{-1}}{\partial t}\right) i_{\text{g-dq0}} - \left(\mathbf{M}\underline{\mathrm{L}}_{\text{abc}}^{-1}\mathbf{M}^{-1}\right) v_{\text{g-dq0}}, \tag{31a}$$

$$\frac{\mathrm{d}v_{\text{g-dq0}}}{\mathrm{d}t} = \left(\mathbf{M}\underline{\mathrm{C}}_{\text{abc}}^{-1}\mathbf{M}^{-1}\right) i_{\text{g-dq0}} - \left(\mathbf{M}\underline{\mathrm{C}}_{\text{abc}}^{-1}\underline{\mathrm{G}}_{\text{abc}}\mathbf{M}^{-1} + \mathbf{M}\frac{\partial \mathbf{M}^{-1}}{\partial t}\right) v_{\text{g-dq0}} - \left(\mathbf{M}\underline{\mathrm{C}}_{\text{abc}}^{-1}\mathbf{M}^{-1}\right) i_{\text{g,g-dq0}}, \tag{31b}$$

$$\frac{\mathrm{d}i_{\text{g,g-dq0}}}{\mathrm{d}t} = \left(\mathbf{M}\underline{\mathrm{L}}_{\text{g,abc}}^{-1}\mathbf{M}^{-1}\right) v_{\text{g-dq0}} - \left(\mathbf{M}\underline{\mathrm{L}}_{\text{g,abc}}^{-1}\underline{\mathrm{R}}_{\text{g,abc}}\mathbf{M}^{-1} + \mathbf{M}\frac{\partial \mathbf{M}^{-1}}{\partial t}\right) i_{\text{g,g-dq0}} - \left(\mathbf{M}\underline{\mathrm{L}}_{\text{g,abc}}^{-1}\mathbf{M}^{-1}\right) v_{\text{g,g-dq0}}. \tag{31c}$$

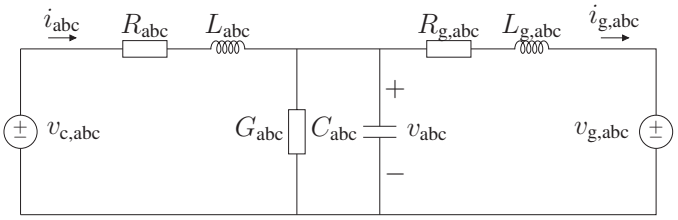

Fig. 1. The grid-connected converter model configuration as in (32).

current flowing through the load, and S_{*} models a load configuration selector, i.e., for single/two/three-phase-to-ground connections and is defined by

$$\mathrm{S}_{*} \in \{\mathrm{S}_{*,\text{a}}, \mathrm{S}_{*,\text{ab}}, \mathrm{S}_{*,\text{abc}}\},$$

where $\mathrm{S}_{*,\text{a}} = \mathrm{diag}(1,0,0)$, $\mathrm{S}_{*,\text{ab}} = \mathrm{diag}(1,1,0)$, and $\mathrm{S}_{*,\text{abc}} = \mathrm{diag}(1,1,1)$. Finally, $v_{\ell,\text{abc}}$ denotes the system voltage at the load connection point. Note that if a diagonal element of S_{*} in (34) is zero, then the corresponding per-phase dynamics is asymptotically stable and converges to zero. Subsequently, one can consider the augmented abc-coordinates dynamics associated with (34), i.e.,

$$\underline{\mathrm{L}}_{\ell,\text{abc}}\frac{\mathrm{d}\underline{i}_{\ell,\text{abc}}}{\mathrm{d}t} = \underline{\mathrm{S}}_{*}\underline{v}_{\ell,\text{abc}} - \underline{\mathrm{R}}_{\ell,\text{abc}}\underline{i}_{\ell,\text{abc}}, \tag{35}$$

similar to (26). Finally, applying the coordinates transformation (18), one can transform (35) to a similar g-dq0 representation as in (29). Note that the formulation in (34) allows to model single/two-phase load connections while preserving the three-phase representation of load dynamics that is essential when applying the g-dq0 transformation. We close by remarking that a star-connected capacitive-conductive load can be modeled following a similar approach.

2) Δ-connection: let us consider a three-phase Δ-connected RL load in abc-coordinates, i.e.,

$$\mathrm{L}_{\ell,\text{ph-ph}}\frac{\mathrm{d}i_{\ell,\text{ph-ph}}}{\mathrm{d}t} = \mathrm{S}_{\Delta}v_{\ell} - \mathrm{R}_{\ell,\text{ph-ph}}i_{\ell,\text{ph-ph}}, \tag{36}$$

where $\mathrm{L}_{\ell,\text{ph-ph}} = \mathrm{diag}(L_{\text{ab}}, L_{\text{bc}}, L_{\text{ca}})$ is assumed to be invertible and $\mathrm{R}_{\ell,\text{ph-ph}} = \mathrm{diag}(R_{\text{ab}}, R_{\text{bc}}, R_{\text{ca}})$, $i_{\ell,\text{ph-ph}}$ denotes the current flowing within the Δ-connected load, S_{Δ} is the load configuration selector, i.e., for single/two/three-phase connection and is defined by

$$\mathrm{S}_{\Delta} \in \{\mathrm{S}_{\Delta,\text{ab}}, \mathrm{S}_{\Delta,\text{ab,bc}}, \mathrm{S}_{\Delta,\text{ab,bc,ca}}\}, \tag{37}$$

where

$$\mathrm{S}_{\Delta,\text{ab}} = \begin{pmatrix} 1 & -1 & 0 \\ 0 & 0 & 0 \\ 0 & 0 & 0 \end{pmatrix},\ \mathrm{S}_{\Delta,\text{ab,bc}} = \begin{pmatrix} 1 & -1 & 0 \\ 0 & 1 & -1 \\ 0 & 0 & 0 \end{pmatrix},\ \text{and}$$

$$\mathrm{S}_{\Delta,\text{ab,bc,ca}} = \begin{pmatrix} 1 & -1 & 0 \\ 0 & 1 & -1 \\ -1 & 0 & 1 \end{pmatrix}.$$

Note that the current absorbed from the system phases by the Δ-connected load can be represented based on the internal load currents, i.e.,

$$i_{\ell,\text{abc}} = \mathbf{T}_{\text{ph-ph}\to\text{ph}}i_{\ell,\text{ph-ph}}, \tag{38}$$

where

$$\mathbf{T}_{\text{ph-ph}\to\text{ph}} = \begin{pmatrix} 1 & 0 & -1 \\ -1 & 1 & 0 \\ 0 & -1 & 1 \end{pmatrix}.$$

To further illustrate, if a Δ-connected load of the form (36) is combined with the system (32) (i.e., connected at the PCC in parallel to the filter capacitive-conductive element), the overall dynamics in abc-coordinates takes the form

$$\mathrm{L}_{\text{abc}}\frac{\mathrm{d}i_{\text{abc}}}{\mathrm{d}t} = v_{\text{c,abc}} - \mathrm{R}_{\text{abc}}i_{\text{abc}} - v_{\text{abc}}, \tag{39a}$$

$$\mathrm{C}_{\text{abc}}\frac{\mathrm{d}v_{\text{abc}}}{\mathrm{d}t} = i_{\text{abc}} - \mathrm{G}_{\text{abc}}v_{\text{abc}} - i_{\ell,\text{abc}} - i_{\text{g,abc}}, \tag{39b}$$

$$\mathrm{L}_{\ell,\text{ph-ph}}\frac{\mathrm{d}i_{\ell,\text{ph-ph}}}{\mathrm{d}t} = \mathrm{S}_{\Delta}v_{\text{abc}} - \mathrm{R}_{\ell,\text{ph-ph}}i_{\ell,\text{ph-ph}}, \tag{39c}$$

$$\mathrm{L}_{\text{g,abc}}\frac{\mathrm{d}i_{\text{g,abc}}}{\mathrm{d}t} = v_{\text{abc}} - \mathrm{R}_{\text{g,abc}}i_{\text{g,abc}} - v_{\text{g,abc}}, \tag{39d}$$

where $i_{\ell,\text{abc}}$ is defined based on (38). Reverting back to the dynamics (36), one can augment the time-domain signals and

parameter matrices as in (26), and derive the augmented Δ-connected load dynamics, i.e.,

$$\underline{\mathrm{L}}_{\ell,\text{ph-ph}} \frac{\mathrm{d}\underline{i}_{\ell,\text{ph-ph}}}{\mathrm{d}t} = \underline{\mathrm{S}}_{\Delta} \underline{v}_{\ell} - \underline{\mathrm{R}}_{\ell,\text{ph-ph}} \underline{i}_{\ell,\text{ph-ph}}. \tag{40}$$

Finally, by applying the (18) allows to transform (40) to a g-dq0 representation that resembles (29). Note that if zero rows of S_{Δ} in (37) sets the voltage difference over the corresponding phase-phase load to zero, thus rendering the phase-phase current dynamics asymptotically stable and converging to zero. Therefore, allowing to model asymmetric phase-phase load connection while preserving the overall three-phase formulation. Last, one can employ the same modeling approach when considering capacitive-conductive Δ-connected load.

We close this section by remarking that the g-dq0 transformation is applicable when considering three-phase unbalanced constant current load models, as well. Further, the case of single/two-phase constant current source models can be investigated by employing the configuration selector formulation as in the case of a star/Δ-connected load. Note that an in-depth systematic investigation on the extension and application of g-dq0 transform for modeling the polyphase (i.e., beyond three-phase) or single/two-phase system is an interesting direction for future research.

V. Simulation Verification

In this section, we consider a simplistic grid-connected converter model of the form (32) that is depicted in Figure 1. Note that here a three-wire converter-grid connection is assumed. We consider (somewhat extreme) non-uniform tolerances of the converter filter parameters, converter and grid voltages as the source of unbalances. In what follows, we verify the equivalence of abc and g-dq0 representations in (32) and (31). Next, we show how a simple proportional-integral (PI)-based control design can be employed in g-dq0 coordinates to balance either the PCC voltage or the grid current.

A. Accuracy verification

Let us begin by investigating the accuracy of g-dq0 transform (18) by comparing the evolution of the dynamical systems (31) and (32). The parameters of the abc-coordinates representation (32) are given in Table I. Further, $\omega^{\star} = 2\pi f^{\star}$, $f^{\star} = 50$ [Hz], and $v^{\star}_{\text{peak}} = 1$ [kV] respectively denote the reference angular frequency, frequency, and peak-per-phase voltage in abc-coordinates. Next, let us consider the converter and grid voltages in (32) (with a similar form to (1)) as

$$v_{\text{c,abc}} = v^{\star}_{\text{peak}} \begin{pmatrix} 1.10\cos\left(\theta_{\text{a}}(t) + \frac{\pi}{10}\right) \\ \cos\left(\theta_{\text{b}}(t)\right) \\ 0.90\cos\left(\theta_{\text{c}}(t) - \frac{\pi}{10}\right) \end{pmatrix},$$

$$v_{\text{g,abc}} = v^{\star}_{\text{peak}} \begin{pmatrix} 0.95\cos\left(\theta_{\text{a}}(t) - \frac{\pi}{5}\right) \\ 1.05\cos\left(\theta_{\text{b}}(t) + \frac{\pi}{5}\right) \\ \cos\left(\theta_{\text{c}}(t)\right) \end{pmatrix}.$$

Figure 2 illustrates the evolution of the trajectories of (31) and (32) under the aforementioned asymmetric circuit parameters and unbalanced converter and grid voltage input characterizations. The results in Figure 2 confirm the exact equivalence of representations (32) and (31). Further, although the abc system is strongly unbalanced the g-dq0 system converges to a stationary equilibrium point. Subsequently, one can perform a linear stability analysis on the g-dq0 system.

TABLE I
Circuit parameters of the grid-connected converter system (32).

Filter RL element [pu]					
R_{a}	R_{b}	R_{c}	L_{a}	L_{b}	L_{c}
0.95	1.00	1.05	0.95	1.00	1.05
Filter GC element [pu]					
G_{a}	G_{b}	G_{c}	C_{a}	C_{b}	C_{c}
1.00	1.10	0.90	1.00	1.10	0.90
Grid RL element [pu]					
$R_{\text{g,a}}$	$R_{\text{g,b}}$	$R_{\text{g,c}}$	$L_{\text{g,a}}$	$L_{\text{g,b}}$	$L_{\text{g,c}}$
1.15	0.85	1.00	1.15	0.85	1.00
Base values					
R_{base}	G_{base}	$R_{\text{g,base}}$	L_{base}	C_{base}	$L_{\text{g,base}}$
1 [mΩ]	10^3 [Ω^{-1}]	10 [mΩ]	100 [μH]	100 [μF]	1 [mH]

B. Proportional-integral balancing control

In this simulation scenario, we consider a simple PI-based balancing control (that is identical for all g-dq0 coordinates) that brings the grid current injection to a balanced three-phase form. To this end, we consider the same parametric characterization as in the previous subsection, however, in this case the converter voltage serves as control input. Let us define the g-dq0-coordinates grid current reference as:

$$i^{\star}_{\text{g,g-dq0}} = (1000, 0, 0, 0, 0, 0)^{\top},$$

and define $e_{i_{\text{g,g-dq0}}} = i^{\star}_{\text{g,g-dq0}} - i_{\text{g,g-dq0}}$. Therefore, with slight abuse of the notation the converter voltage is given by:

$$v_{\text{c,g-dq0}} = \kappa_{\text{p}} e_{i_{\text{g,g-dq0}}} + \kappa_{\text{i}} \int_0^t e_{i_{\text{g,g-dq0}}} \mathrm{d}\tau. \tag{42}$$

We combine (42) with (31), and transform $v_{\text{c,g-dq0}}$ in (42) to the abc-coordinates and apply it as an input to (32). The resulting evolution of the abc and g-dq0 systems under the balancing control (42), with $\kappa_{\text{p}} = 1$ and $\kappa_{\text{i}} = 50$ is illustrated in Figure 3. As it is shown in Figure 3, the simplistic PI-based current balancing control design in (42) exhibits satisfactory performance that further highlights the benefit of utilizing g-dq0-coordinates transformation (see the $i_{\text{g,g-dq0}}$ evolution under the balancing control and its abc-coordinates image). Following a similar approach one can implement a PCC voltage balancing control, as well.

VI. Conclusion and Outlook

In this paper, we provided a review of the modeling and analysis methods for the unbalanced systems. Next, starting

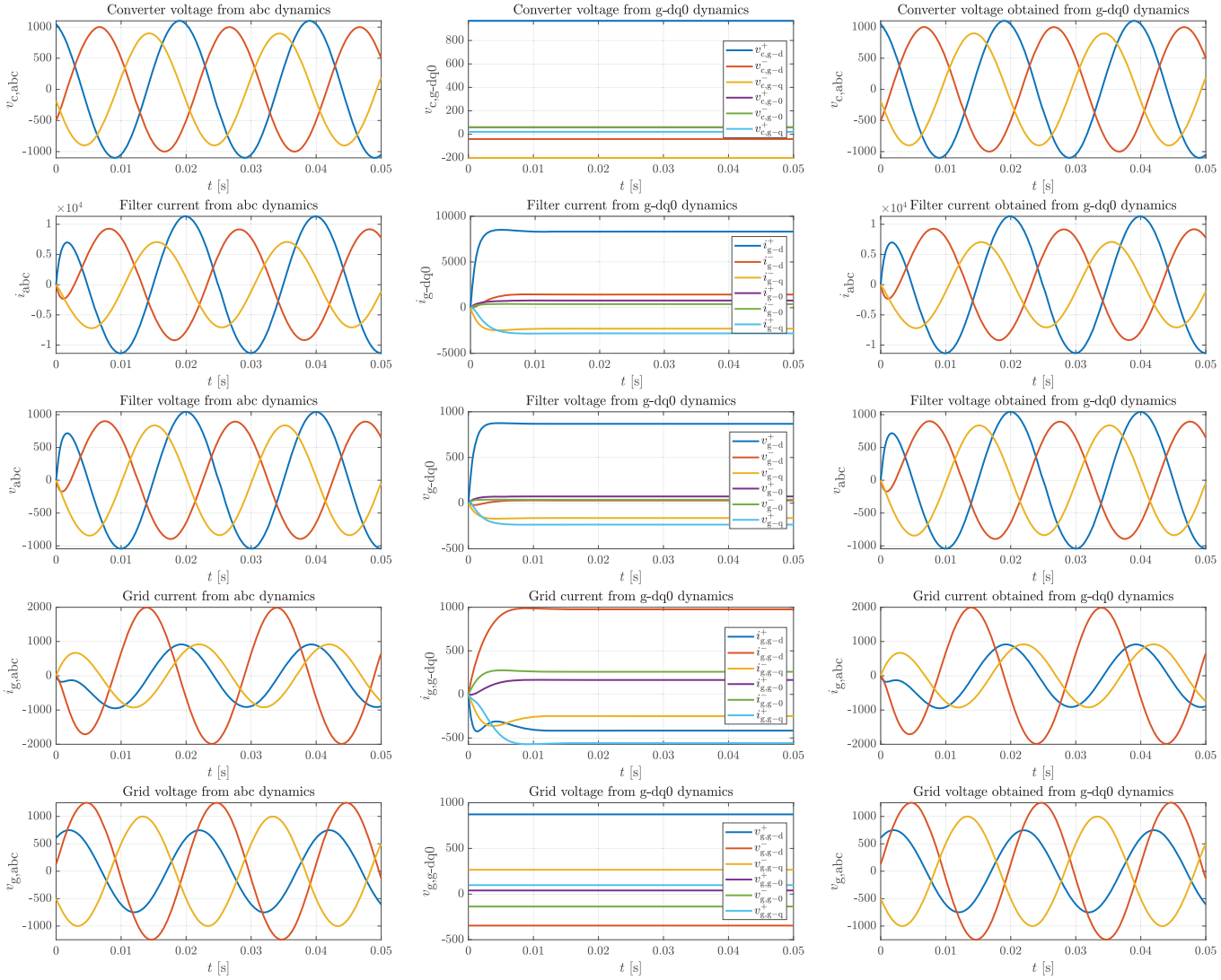

Fig. 2. The time-evolution of system trajectories under the parameter and input characterization is Subsection V-A: abc-coordinates dynamics (32) (left), the g-dq0-coordinates dynamics (31) (middle), and abc-coordinates signals constructed based on the evolution of the g-dq0 dynamics (31) by utilizing the inverse transformation (18) (right).

from a previously proposed time-domain modeling framework, we derived a generalized variant of the standard dq0 transformation, that is termed g-dq0 transform. Further, we investigated the mathematical properties of this transformation and explored its application to the dynamic circuit element modeling. We provided an example of converter-based systems accompanied by details on unbalanced load modeling. Finally, a simulation-based accuracy verification was presented and a simplistic balancing control design was discussed. Our agenda of future work includes: extending the modeling approach to more complex converter configurations (possibly with a four-wire connection and exploring the impact of zero-sequence flow), considering detailed converter model with either star or delta connection, theoretic extension of the proposed transform for single/two-phase or polyphase systems, exploring the transform application while considering the DC converter dynamics, more complex control design for the unbalanced systems based on the g-dq0 transform, and simulation-based case studies of the fault ride through behavior and harmonics modeling when utilizing the g-dq0 transform.

Appendix

Proof of Proposition 1. Let us expend the LHS of (12) as

$$\left(\sum_{j=1}^{n} Y_j \cos\phi_j\right)\cos\omega t - \left(\sum_{j=1}^{n} Y_j \sin\phi_j\right)\sin\omega t. \quad (43)$$

The time-invariant coefficients in (43) can take the form

$$\sum_{j=1}^{n} Y_j \cos\phi_j = Y\cos\phi \quad \text{and} \quad \sum_{j=1}^{n} Y_j \sin\phi_j = Y\sin\phi, \quad (44)$$

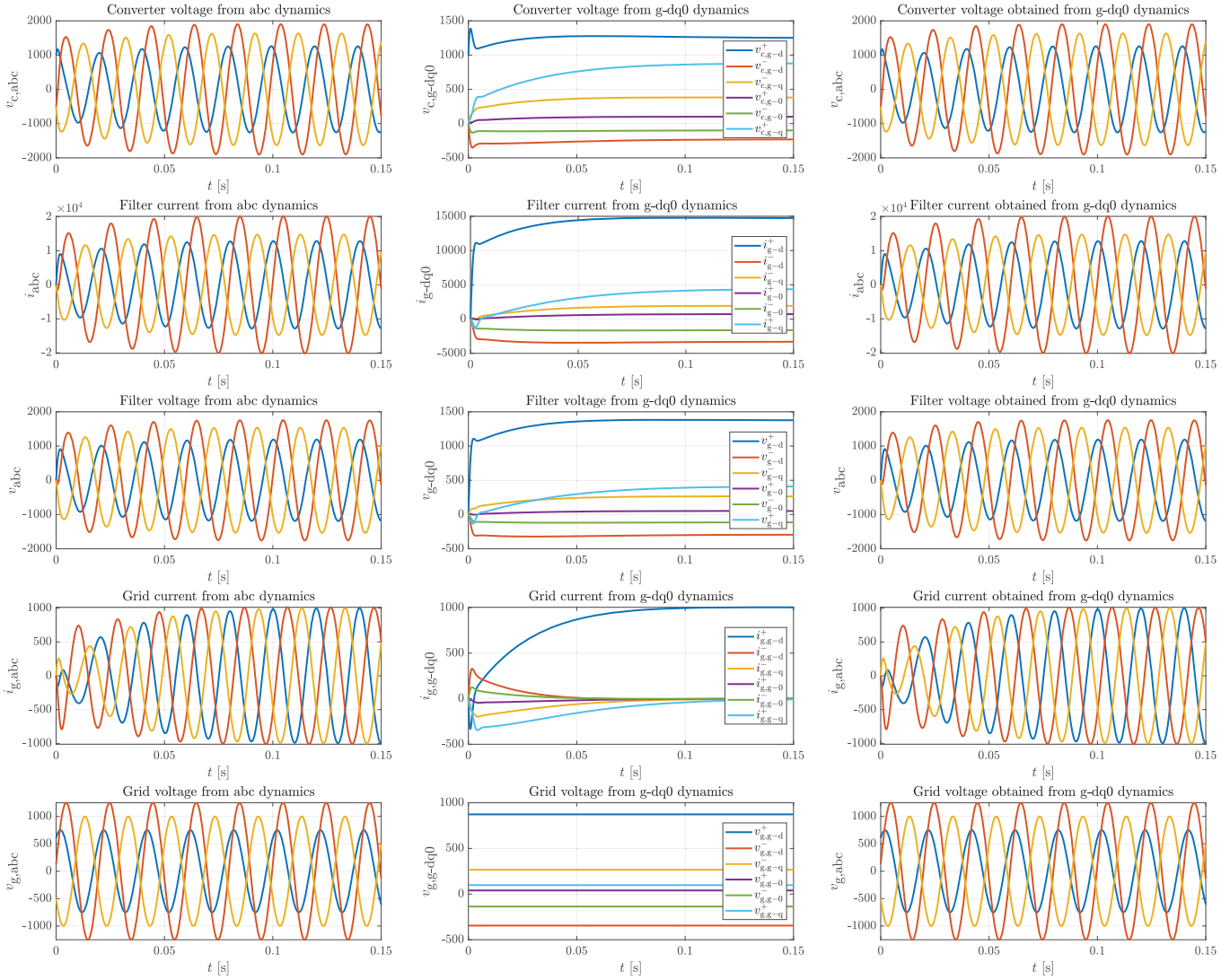

Fig. 3. The time-evolution of system trajectories under the parameter and input characterization is Subsection V-A and the current-balancing control (42): abc-coordinates dynamics (32) (left), the g-dq0-coordinates dynamics (31) (middle), and abc-coordinates signals constructed based on the evolution of the g-dq0 dynamics (31) by utilizing the inverse transformation (18) (right).

where straightforward trigonometric computations yields the expressions in (13) for Y and ϕ. Finally, replacing the coefficients in (43) with the expressions in the RHSs of (44) and exploiting the angle sum trigonometric identity, one can derive the expression in the RHS of (12). □

Proof of Proposition 2. If $\mathrm{P}_{\mathbf{T}}$ is constant then

$$\frac{\partial \mathrm{P}_{\mathbf{T}}}{\partial t} = \frac{\partial \left(\mathbf{T}\mathrm{P}\mathbf{T}^{-1}\right)}{\partial t} = \frac{\partial \mathbf{T}}{\partial t}\mathrm{P}\mathbf{T}^{-1} + \mathbf{T}\mathrm{P}\frac{\partial \mathbf{T}^{-1}}{\partial t} = \mathbf{0}_{n\times n}. \quad (45)$$

Note that $\mathbf{T}$ is invertible, i.e., $\mathbf{T}\mathbf{T}^{-1} = \mathbf{I}_n$, therefore

$$\frac{\partial \left(\mathbf{T}\mathbf{T}^{-1}\right)}{\partial t} = \frac{\partial \mathbf{T}}{\partial t}\mathbf{T}^{-1} + \mathbf{T}\frac{\partial \mathbf{T}^{-1}}{\partial t} = \frac{\partial \mathbf{I}_n}{\partial t} = \mathbf{0}_{n\times n}, \quad (46)$$

which means

$$\frac{\partial \mathbf{T}}{\partial t} = -\mathbf{T}\frac{\partial \mathbf{T}^{-1}}{\partial t}\mathbf{T}. \quad (47)$$

Replacing $\partial\mathbf{T}/\partial t$ in (45) with (47) results in

$$\frac{\partial \mathrm{P}_{\mathbf{T}}}{\partial t} = -\mathbf{T}\left(\frac{\partial \mathbf{T}^{-1}}{\partial t}\mathbf{T}\mathrm{P}\right)\mathbf{T}^{-1} + \mathbf{T}\mathrm{P}\frac{\partial \mathbf{T}^{-1}}{\partial t} = \mathbf{0}_{n\times n}, \quad (48)$$

which always holds if condition (24) is satisfied. □

References

[1] F. Milano, F. Dörfler, G. Hug, D. J. Hill, and G. Verbič, "Foundations and challenges of low-inertia systems (invited paper)," in *Power Systems Computation Conference (PSCC)*, 2018, pp. 1–25.

[2] A. Tayyebi, D. Groß, A. Anta, F. Kupzog, and F. Dörfler, "Frequency stability of synchronous machines and grid-forming power converters," *IEEE Journal of Emerging and Selected Topics in Power Electronics*, vol. 8, no. 2, pp. 1004–1018, 2020.

[3] N. Hatziargyriou, J. Milanovic, C. Rahmann, V. Ajjarapu, C. Canizares, I. Erlich, D. Hill, I. Hiskens, I. Kamwa, B. Pal *et al.*, "Definition and classification of power system stability–revisited & extended," *IEEE Transactions on Power Systems*, vol. 36, no. 4, pp. 3271–3281, 2020.

[4] R. Henriquez-Auba, J. D. Lara, D. S. Callaway, and C. Barrows, "Transient simulations with a large penetration of converter-interfaced generation: scientific computing challenges and opportunities," *IEEE Electrification Magazine*, vol. 9, no. 2, pp. 72–82, 2021.

[5] B. Shakerighadi, N. Johansson, R. Eriksson, P. Mitra, A. Bolzoni, A. Clark, and H.-P. Nee, "An overview of stability challenges for power-electronic-dominated power systems: The grid-forming approach," *IET Generation, Transmission & Distribution*, vol. 17, no. 2, pp. 284–306, 2023.

[6] A. Crivellaro, A. Tayyebi, C. Gavriluta, D. Groß, A. Anta, F. Kupzog, and F. Dörfler, "Beyond low-inertia systems: Massive integration of grid-forming power converters in transmission grids," in *IEEE Power & Energy Society General Meeting (PESGM)*, 2020, pp. 1–5.

[7] M. Lu, S. Dhople, and B. Johnson, "Benchmarking nonlinear oscillators for grid-forming inverter control," *IEEE Transactions on Power Electronics*, vol. 37, no. 9, pp. 10 250–10 266, 2022.

[8] "Voluntary specification for grid-forming inverters," Australian Energy Market Operator (AEMO), Tech. Rep., 2023.

[9] "Great Britain grid-forming best practice guide," National Grid Electricity System Operator (ESO), Tech. Rep., 2023.

[10] A. Stankovic and T. Aydin, "Analysis of asymmetrical faults in power systems using dynamic phasors," *IEEE Transactions on Power Systems*, vol. 15, no. 3, pp. 1062–1068, 2000.

[11] Z. Li, S.-C. Wong, C. K. Tse, and X. Liu, "Modeling of unbalanced three-phase driving-point impedance with application to control of grid-connected power converters," *International Journal of Circuit Theory and Applications*, vol. 44, no. 4, pp. 851–873, 2016.

[12] C. L. Fortescue, "Method of symmetrical co-ordinates applied to the solution of polyphase networks," *Transactions of the American Institute of Electrical Engineers*, vol. 37, no. 2, pp. 1027–1140, 1918.

[13] I. Džafić, B. C. Pal, M. Gilles, and S. Henselmeyer, "Generalized π fortescue equivalent admittance matrix approach to power flow solution," *IEEE Trans. Power Syst.*, vol. 29, no. 1, pp. 193–202, 2013.

[14] Y. Ojo and J. Schiffer, "Towards a time-domain modeling framework for small-signal analysis of unbalanced microgrids," in *IEEE PowerTech Conference*, 2017.

[15] S. J. Yague, A. García-Cerrada, and P. P. Farré, "Comparison between modal analysis and impedance-based methods for analysing stability of unbalanced microgrids with grid-forming electronic power converters," *Journal of Modern Power Systems and Clean Energy*, vol. 11, no. 4, pp. 1269–1281, 2023.

[16] D. Jovcic, *High voltage direct current transmission: converters, systems and DC grids*. John Wiley & Sons, 2019.

[17] R. Teodorescu, M. Liserre, and P. Rodriguez, *Grid converters for photovoltaic and wind power systems*. John Wiley & Sons, 2011.

[18] H. Akagi, E. H. Watanabe, and M. Aredes, *Instantaneous power theory and applications to power conditioning*. John Wiley & Sons, 2017.

[19] A. Yazdani and R. Iravani, *Voltage-sourced converters in power systems: modeling, control, and applications*. John Wiley & Sons, 2010.

[20] C. J. O'Rourke, M. M. Qasim, M. R. Overlin, and J. L. Kirtley, "A geometric interpretation of reference frames and transformations: dq0, clarke, and park," *IEEE Trans. Energy Convers.*, vol. 34, no. 4, pp. 2070–2083, 2019.

[21] Y. Zhou, P. Bauer, J. A. Ferreira, and J. Pierik, "Operation of grid-connected DFIG under unbalanced grid voltage condition," *IEEE Trans. Energy Convers.*, vol. 24, no. 1, pp. 240–246, 2009.